Journal of Alzheimer's Disease 78 (2020) 1149–1159
DOI 10.3233/JAD-200520
IOS Press

Impairment of Everyday Spatial Navigation Abilities in Mild Cognitive Impairment Is Weakly Associated with Reduced Grey Matter Volume in the Medial Part of the Entorhinal Cortex

Asma Hallab[a], Catharina Lange[a], Ivayla Apostolova[b], Cansu Özden[b], Gabriel Gonzalez-Escamilla[c,d], Susanne Klutmann[b], Winfried Brenner[a], Michel J. Grothe[c,e] and Ralph Buchert[b,*] for the Alzheimer's Disease Neuroimaging Initiative[1]

[a]*Department of Nuclear Medicine, Charité - Universitätsmedizin Berlin, Corporate Member of Freie Universität Berlin, Humboldt-Universität zu Berlin, and Berlin Institute of Health, Berlin, Germany*

[b]*Department of Diagnostic and Interventional Radiology and Nuclear Medicine, University Medical Center Hamburg-Eppendorf, Hamburg, Germany*

[c]*German Center for Neurodegenerative Diseases (DZNE), Rostock/Greifswald, Rostock, Germany*

[d]*Department of Neurology, University Medical Center of the Johannes Gutenberg University Mainz, Mainz, Germany*

[e]*Unidad de Trastornos del Movimiento, Servicio de Neurología y Neurofisiología Clínica, Instituto de Biomedicina de Sevilla, Hospital Universitario Virgen del Rocío/CSIC/Universidad de Sevilla, Seville, Spain*

Accepted 15 September 2020

Abstract.

Background: Research in rodents identified specific neuron populations encoding information for spatial navigation with particularly high density in the medial part of the entorhinal cortex (ERC), which may be homologous with Brodmann area 34 (BA34) in the human brain.

Objective: The aim of this study was to test whether impaired spatial navigation frequently occurring in mild cognitive impairment (MCI) is specifically associated with neurodegeneration in BA34.

Methods: The study included baseline data of MCI patients enrolled in the Alzheimer's Disease Neuroimaging Initiative with high-resolution structural MRI, brain FDG PET, and complete visuospatial ability scores of the Everyday Cognition test (VS-ECog) within 30 days of PET. A standard mask of BA34 predefined in MNI space was mapped to individual native space to determine grey matter volume and metabolic activity in BA34 on MRI and on (partial volume corrected) FDG PET, respectively. The association of the VS-ECog sum score with grey matter volume and metabolic activity in BA34, *APOE4* carrier status, age, education, and global cognition (ADAS-cog-13 score) was tested by linear regression. BA28, which constitutes the lateral part of the ERC, was used as control region.

[1]Data used in preparation of this article were obtained from the Alzheimer's Disease Neuroimaging Initiative (ADNI) database (https://www.loni.ucla.edu/ADNI). As such, the investigators within ADNI contributed to the design and implementation of ADNI and/or provided data but did not participate in analysis or writing of this paper. A complete listing of ADNI investigators can be found at: https://adni.loni.ucla.edu/wp-content/uploads/how_to_apply/ADNI_Acknowledgement_List.pdf.

*Correspondence to: Ralph Buchert, Martinistr. 52, 20246 Hamburg, Germany. Tel.: +49 40 741054347; Fax: +49 40 7410 40265; E-mail: r.buchert@uke.de.; ORCID ID 0000-0002-0945-0724

Results: The eligibility criteria led to inclusion of 379 MCI subjects. The VS-ECog sum score was negatively correlated with grey matter volume in BA34 ($\beta = -0.229$, $p = 0.022$) and age ($\beta = -0.124$, $p = 0.036$), and was positively correlated with ADAS-cog-13 ($\beta = 0.175$, $p = 0.003$). None of the other predictor variables contributed significantly.
Conclusion: Impairment of spatial navigation in MCI is weakly associated with BA34 atrophy.

Keywords: Entorhinal cortex, ^{18}F-fluorodeoxyglucose, grid cells, magnetic resonance imaging, mild cognitive impairment, positron emission tomography, spatial navigation, volumetry

INTRODUCTION

Volumetric brain analyses based on structural magnetic resonance imaging (MRI) and assessment of regional cerebral glucose metabolism by positron emission tomography (PET) with the glucose analog ^{18}F-fluorodeoxyglucose (FDG) as surrogate marker of signaling-related synaptic activity [1] have been widely used to study associations between neurodegeneration/neuronal dysfunction and cognition [2, 3]. Many MRI studies have focused on hippocampus atrophy and its relationship with memory performance [4–9]. Other brain regions and other cognitive domains are less well studied.

The entorhinal cortex (ERC), which constitutes the anterior part of the parahippocampal gyrus in the medial temporal lobe, serves as a gateway providing input from frontal, parietal, occipital, and other parts of the temporal cortex to the hippocampus [10–12]. Research in rodents identified spatially modulated neurons such as grid and head direction cells that encode information for spatial navigation and that are primarily located in the medial part of the ERC [13–15]. The lateral ERC primarily supports temporal orientation [16] as well as olfactory and somatosensory processing [17, 18].

A study on the functional topography of the ERC in humans using high-field, high-resolution functional MRI during a virtual reality task with spatial and non-spatial stimuli identified two clusters in the ERC with different connectivity patterns [12]. One cluster was more strongly connected to a posterior-medial network, including occipital and posterior-parietal cortex, that was sensitive to spatial stimuli [12]. This cluster was located more medially comprising parts of the ERC that may be approximated by Brodmann area 34 (BA34) [19]. The second cluster was more strongly connected to an anterior-temporal network, including medial-prefrontal and orbitofrontal cortex, that was sensitive to non-spatial stimuli [12]. This cluster was located more laterally comprising parts of the ERC that may be approximated by BA28. These findings suggest that BA34 is the human homologue of the medial ERC in rodents and may therefore be particularly involved in spatial navigation tasks.

Against this background, the present study focused on BA34 and spatial navigation in patients with mild cognitive impairment (MCI). MCI is defined by the occurrence of cognitive impairment that can be verified by neuropsychological testing, but is not severe enough to clearly affect activities of daily living [20, 21]. Deficits in spatial navigation are frequent in MCI [22, 23]. MCI can have various causes including neurodegenerative, cerebrovascular, mixed (neurodegenerative plus cerebrovascular), and non-neurodegenerative diseases [24]. ERC atrophy is more frequent in MCI patients compared to healthy controls and constitutes a risk factor for MCI-to-dementia progression [25]. In the present study, MCI was considered a general "lesion model" of spatial navigation deficits and ERC degeneration/dysfunction, independent of the underlying etiology.

Neuronal loss and synaptic dysfunction in BA34 were assessed by MRI-based volumetry and FDG PET, respectively. Spatial navigation abilities were characterized by the self-reported visuospatial subscores of the Everyday Cognition questionnaire (VS-ECog) [26]. BA28 was used as control region.

The hypothesis put to test was that VS-ECog performance is associated with the grey matter volume specifically in BA34 (rather than BA28) and that (partial volume corrected) FDG uptake specifically in BA34 is an independent (of grey matter volume) predictor of VS-ECog performance.

MATERIALS AND METHODS

MCI patients

Baseline data of 458 Alzheimer's Disease Neuroimaging Initiative (ADNI) MCI subjects (mean age 71.7 ± 7.4 years, 45.2% females, 47.8% *APOE4*-positive) with MPRAGE MRI, brain FDG PET and VS-ECog scores were downloaded from the ADNI repository (https://adni.loni.usc.edu/).

The ADNI is a longitudinal multicenter study aimed at investigating whether neuroimaging methods such as MRI and PET, together with genetic, clinical and neuropsychological measures can be used to characterize progression of MCI and Alzheimer's disease (AD). The ADNI was launched in 2003 as a public-private partnership, led by Principal Investigator Michael W. Weiner, MD. The primary goal of ADNI has been to test whether serial MRI, PET, other biological markers, and clinical and neuropsychological assessment can be combined to measure the progression of MCI and early AD.

Grey matter volume in BA34 and BA28

MR images were segmented using the unified segmentation method [27] implemented in the Statistical Parametric Mapping software package (version SPM12, Wellcome Trust Centre for Neuroimaging, London, UK) with default parameter settings except that image data was sampled to 2 mm [28]. The unified segmentation approach yields individual probability maps of grey matter, white matter and cerebrospinal fluid.

Bilateral binary masks of BA34 and BA28 predefined in the anatomical space of the Montreal Neurological Institute (MNI) by the TD Brodmann areas atlas in the PickAtlas-tool (Wake Forest University [29, 30]) were transformed into individual patient space using the inverse of the transformation from individual patient space to MNI space estimated by unified segmentation. Grey matter volume in BA34 or BA28 was calculated by voxelwise multiplying the patient's grey matter probability map from SPM segmentation with the transformed BA mask, then summing over all voxel intensities, and finally multiplying the sum by the volume of a single voxel. A grey matter probability threshold was not applied.

Glucose metabolism in BA34 and BA28

Multicentric FDG PET acquisition in ADNI follows different scanner-specific acquisition protocols starting 30 min post injection and acquiring either 6 frames of 5 min duration or 33 frames of 1 min duration or a single static scan of 30 min duration. Image reconstruction is performed with scanner-specific reconstruction algorithms but harmonized parameter settings to achieve similar image quality at all centers. Acquisition and reconstruction parameters for each PET scanner are given in the ADNI PET procedure manual (https://adni.loni.usc.edu/wp-content/uploads/2010/09/PET-Tech_Procedures_Manual_v9.5.pdf). Reconstructed dynamic (or static, if dynamic not available) PET data was downloaded in its original image format ("as archived", DICOM, Interfile, or ECAT) in order to guarantee that no preprocessing had been performed. Then, the original images were converted to Nifti file format using SPM8 for DICOM and ECAT formats and ImageConverter (version 1.1.5) for Interfile format. In dynamic FDG PETs, inter-frame motion was detected using the Realign-tool of SPM8. The first frame was used as reference and the magnitude of the motion of subsequent frames relative to the reference frame was estimated by tracking five reference points within the brain as described previously [31]. PET frames with a motion amplitude larger than 4 mm were discarded [32]. A motion-corrected static FDG uptake image was obtained by summing all remaining frames (with motion amplitude $\leq$4 mm) after realignment [31]. The FDG uptake image was co-registered to the individual MRI using the Coregister-tool of SPM8.

MRI-based PVE correction was performed using the Müller-Gärtner method implemented in the SPM toolbox PETPVE12 and an isotropic Gaussian kernel with 7 mm full-width-at-half-maximum [33]. Mean PVE-corrected FDG uptake in BA34 or BA28 was obtained by the weighted average of the voxelwise PVE-corrected FDG uptake over all voxels in the BA34 or BA28 mask in patient space. The individual grey matter probability map from segmentation was used for the weighting of voxels, that is, the PVE-corrected FDG uptake in a given voxel in BA34 or BA28 was weighted by the grey matter probability of this voxel. Mean PVE-corrected FDG uptake in BA34 and BA28 was scaled to the mean non-PVE-corrected FDG uptake in the pons [34]. In the following, "FDG uptake" always means "mean PVE-corrected FDG uptake scaled to mean non-PVE-corrected FDG uptake in the pons". Patients in whom the pons was not fully included in the axial field-of-view of the PET scan were excluded.

Spatial navigation performance

Spatial navigation performance was characterized by the sum of the following self-reported VS-ECog subcores: following a map to find a new location (VISSPAT1), reading a map and helping with directions when someone else is driving (VISSPAT2), finding my car in a parking lot (VISSPAT3), finding my way back to a meeting spot in the mall or other

location (VISSPAT4), finding my way around a familiar neighborhood (VISSPAT6), same with familiar store (VISSPAT7), and same with house visited many times (VISSPAT8) [26]. The VISSPAT5 subscore was not included, because it was not available in the majority of patients. Each subscore ranged from 0 ("better or no change compared to 10 years earlier") to 3 ("consistently much worse compared to 10 years earlier"). The sum score ranged from 0 to 21 (0: normal, 21: most strongly impaired).

Maximum allowed delay between FDG PET and ECog testing was 30 days. Patients with longer delay were excluded.

Statistical analysis

Outliers were removed in order to reduce the risk of false positive findings driven by outliers. A patient was considered an outlier if it differed by more than three standard deviations from the mean with respect to one or more of the following variables: grey matter volume of BA34, grey matter volume of BA28, FDG uptake in BA34, FDG uptake in BA28. In addition, patients who differed more than three standard deviations from the regression line of PVE-corrected FDG uptake versus non-PVE-corrected FDG uptake in at least one of the two regions (BA34, BA28) were also excluded. The rationale for this was to exclude cases with high probability of PVE over-correction.

The primary statistical analysis of this study was linear regression of the "continuous" VS-ECog sum score with the following set of predictor variables: grey matter volume in BA34, grey matter volume in BA28, FDG uptake in BA34, FDG uptake in BA28, *APOE4* carrier status (positive or negative), age, years of education, and overall cognitive performance. The latter was characterized by the 13 items cognitive subscale of the Alzheimer's Disease Assessment Scale (ADAS-cog-13). Regression analysis was performed with all predictors entered in the equation or with backward elimination (entry $p = 0.050$, removal $p = 0.075$). Regression analysis was first performed in all MCI patients and then separately in the subgroup of MCI patients with impaired spatial navigation (VS-ECog sum score > cutoff) and in the subgroup of MCI patients with relatively preserved spatial navigation (VS-ECog sum score $\leq$ cutoff).

Sex was not included as covariate in the regression analyses, although there is considerable evidence that spatial navigation is a sexually dimorphic skill [35]. However, the VS-ECog compares the current performance in everyday spatial navigation tasks to the performance 10 years earlier [26]. Thus, each subject serves as its own control, which is assumed to eliminate relevant sex differences. In line with this, development and validation of the ECog did not include sex as a relevant covariate, in contrast to age and education [26].

VS-ECog performance was dichotomized as "impaired" or "relatively preserved" by using the median value of the VS-ECog sum score amongst the included patients as cutoff. Classification and regression tree analysis of the dichotomized VS-ECog sum score was performed with grey matter volume in BA34, age, and ADAS-cog-13 as continuous predictor variables. An 80%-to-20% random split into training and test sample was used to avoid overly optimistic performance estimates due to overfitting. The depth of the tree was fixed to 2, the minimum number of cases was set to 50/25 for parent/child nodes. Minimum change of improvement was set to 0.0001.

In order to further characterize the effects detected by regression and decision tree analysis, two-way multivariate analysis of covariance (MANCOVA) of grey matter volume and FDG uptake in BA34 combined as dependent variables was performed with dichotomized VS-ECog and *APOE4* carrier status as fixed factors, and age at PET, ADAS-cog-13, and years of education as covariates. The estimated marginal mean of the dependent variables was used to characterize the percentage difference of the dependent variables between impaired and relatively preserved spatial navigation. A second two-way MANCOVA with the same fixed factors and the same covariates was performed with grey matter volume and FDG uptake in BA28 combined as dependent variables. Each two-way MANCOVA was complemented by two follow-up two-way univariate analyses of covariance (ANCOVA) to test specifically for the effect of either FDG uptake or grey matter volume alone.

Additional MANCOVAs with spatial navigation performance dichotomized by k-means clustering of the seven VS-ECog subscores (VISSPAT 1–4, 5–8) as fixed factor are given in the Supplementary Material.

In order to assess the utility of the VS-ECog to predict BA34 atrophy in MCI patients, stepwise regression analysis of the grey matter volume in BA34 was performed with total intracranial volume (TIV), age, ADAS-cog-13, and the "continuous" VS-ECog sum score as predictor variables. TIV was estimated by the sum of the total volume of grey matter, total volume of white matter, and total volume of cerebrospinal fluid. The total volume of a given

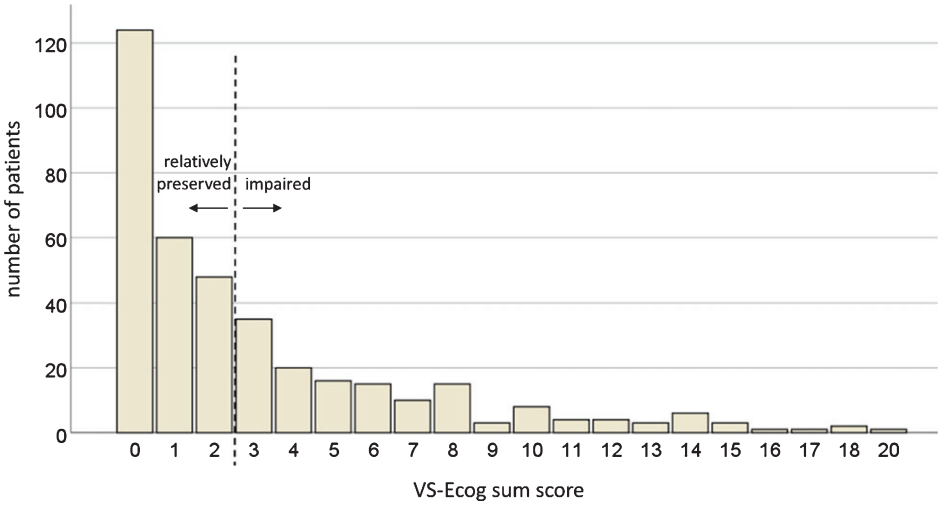

Fig. 1. Distribution of the VS-ECog sum score in the included MCI patients.

component was computed by the sum of all voxel intensities in the corresponding individual probability map from the SPM segmentation multiplied by the voxel volume.

Adjusted R^2, that is, the proportion of the variance of the dependent variable that was explained by the model was used to characterize effect sizes. The change of adjusted R^2 was used to characterize the effect size of the contribution of individual predictor variables.

All statistical analyses were performed using SPSS (version 25, IBM Corporation).

RESULTS

One or more exclusion criteria were met by 79 of the 458 patients (17.2%). No patient was excluded due to incomplete coverage of the pons in the PET scan, 15 patients (3.3%) were outliers with respect to grey matter volume and/or FDG uptake in BA34, 14 patients (3.1%) were outliers with respect to grey matter volume and/or FDG uptake in BA28, in 33 patients (7.2%) the delay between FDG PET and VS-ECog testing was longer than 30 days, and at least one of the VS-ECog subscores was missing in 32 patients (7.0%).

The remaining 379 patients were included in the analyses (mean age 71.5 ± 7.4 years, range 55–91 years; 43.0% females; 48.3% *APOE4*-positive; 16.3 ± 2.6 years of education, range 10–20 years; ADAS-cog-13 14.8 ± 6.7, range 2–38).

The distribution of the VS-ECog sum score amongst the included patients is shown in Fig. 1. The median value of the VS-ECog sum score was 2. Using this value as cutoff, 147 patients (38.8%) were categorized as impaired (VS-ECog sum score >2) with respect to spatial navigation, the remaining 232 patients (61.2%) were categorized as relatively preserved (VS-ECog sum score $\leq$2).

Linear regression of the "continuous" VS-ECog sum score in the whole group of MCI patients and with entering all predictor variables revealed a significant model ($F = 2.792$, $p = 0.005$) that explained 3.7% of the variance of the VS-ECog sum score (adjusted $R^2 = 0.037$). The following predictors contributed significantly: grey matter volume in BA34 (standardized coefficient $\beta = -0.229$, $p = 0.022$), age ($\beta = -0.124$, $p = 0.036$), and ADAS-cog-13 ($\beta = 0.175$, $p = 0.003$). The remaining predictors did not contribute significantly (Table 1). This finding was confirmed by linear regression with backward elimination that only kept grey matter volume in BA34 ($\beta = -0.149$, $p = 0.014$), age ($\beta = -0.129$, $p = 0.027$), and ADAS-cog-13 ($\beta = 0.142$, $p = 0.010$) in the model ($F = 6.004$, $p = 0.001$; adjusted $R^2 = 0.038$). When linear regression of the "continuous" VS-ECog sum score was restricted to the subgroup of MCI patients with impaired spatial navigation (VS-ECog sum score >2), backward elimination left only grey matter volume in BA34 in the model (ANOVA: $F = 5.649$, $p = 0.019$; age: $\beta = -0.194$, $p = 0.019$; adjusted $R^2 = 0.031$). Neither age nor ADAS-cog-13 was included in this case. In the subgroup of MCI patients with relatively preserved spatial navigation (VS-ECog sum score $\leq$2), backward elimination removed all predictor

Table 1
Linear regression of the "continuous" sum score of the visuospatial domain ECog subtest (VS-ECog) with grey matter volume and FDG uptake in BA34, grey matter volume and FDG uptake in BA28, *APOE4* carrier status (positive or negative), age at PET, years of education and ADAS-cog-13 as covariates. All predictor variables were entered in the model. (β, standardized regression coefficient; *p*, significance)

	grey matter BA34	FDG uptake BA34	grey matter BA28	FDG uptake BA28	*APOE4*	age	ADAS-cog-13	education
β	–0.229	–0.055	0.059	0.137	–0.023	–0.124	0.175	-0.010
p	**0.022**	0.469	0.558	0.106	0.657	**0.036**	**0.003**	0.841

variables, including grey matter volume in BA34, that is, only the constant remained in the model.

The decision tree analysis of the dichotomized VS-ECog sum score selected grey matter volume in BA34 with 0.75 ml cutoff for branching at the root level (Supplementary Figure 3). In the training set, the proportion of patients with impaired spatial navigation increased from 40.6% in the whole training set to 56.4% in patients with BA34 grey matter volume $\leq$0.75 ml, and it decreased to 37.0% in patients with BA34 grey matter volume >0.75 ml. ADAS-cog-13 with 15.5 points as cutoff was selected for second level branching of patients with relatively preserved BA34 grey matter volume. The proportion of patients with impaired spatial navigation increased from 37.0% to 47.7% in the MCI patients with more impaired ADAS-cog-13 performance, it decreased to 30.7% in the MCI patients with better ADAS-cog-13 score. The model did not include second level branching of patients with more strongly decreased BA34 grey matter volume. The same trends were observed in the test set (Supplementary Figure 3). Classification accuracy in the test set was 62.8% (Supplementary Figure 3), smaller than the proportion of patients with relatively preserved spatial navigation performance in the test set (67.4%).

The results of the two-way MANCOVA of grey matter volume and FDG uptake in BA34 combined as dependent variables with dichotomized VS-ECog and *APOE4* carrier status as fixed factors, and age at PET, ADAS-cog-13, and years of education as covariates are summarized in Table 2. The effect of the dichotomized VS-ECog sum score on the dependent variables slightly missed statistical significance in the multivariate analysis ($p = 0.079$). In the follow-up ANCOVAs, the effect of BA34 grey matter volume reached statistical significance ($p = 0.037$, not corrected for multiple testing; adjusted $R^2 = 0.297$), while the effect of FDG uptake in BA34 clearly failed to reach significance ($p = 0.552$; adjusted $R^2 = 0.048$). The estimated marginal mean of the BA34 grey matter volume was about 3.3% smaller in the MCI patients with impaired spatial navigation compared to the MCI patients with relatively preserved spatial navigation (0.868 ± 0.011 ml versus 0.898 ± 0.009 ml, Table 2). The association between the two dependent variables with age and ADAS-cog-13 was highly statistically significant in the multivariate and in both univariate analyses ($p < 0.003$) except for the association of FDG uptake in BA34 with age ($p = 0.343$). The association of the dependent variables with years of education reached borderline significance or trend level in all analyses ($0.027 \leq p \leq 0.071$, Table 2).

The results of the two-way MANCOVA of grey matter volume and FDG uptake in BA28 combined are summarized in Table 2. The grey matter volume in BA28 was also smaller in MCI patients with impaired spatial navigation, but the difference did not reach statistical significance in the univariate analysis ($p = 0.121$, Table 2).

The stepwise regression of BA34 grey matter volume with TIV, age, ADAS-cog-13 and the "continuous" VS-ECog sum score as predictor variables resulted in a highly significant model ($F = 55.0$, $p < 0.0005$) that explained 36.4% (adjusted R^2) of the variance of BA34 grey matter volume. Age alone explained 23.2% of the variance of BA34 grey matter volume, age and ADAS-cog-13 combined explained 29.0%, age and ADAS-cog-13 and TIV combined explained 36.0%, and age and ADAS-cog-13 and TIV and VS-ECog sum score combined explained 36.4% of the variance of BA34 grey matter volume (adjusted R^2 at each step). Thus, the VS-ECog sum score explained only 0.4% of the variance of BA34 grey matter volume beyond age, ADAS-cog-13, and TIV. The change of the F statistic was highly significant when age, ADAS-cog-13, and TIV were added successively to the regression model (all $p < 0.0005$), it reached trend level when the VS-ECog sum score was added ($p = 0.081$).

DISCUSSION

The primary finding of this study was the association between worse spatial navigation performance

Table 2
Two-ways multivariate analysis of covariance (MANCOVA) of either grey matter volume and FDG uptake in BA34 combined as dependent variables or grey matter volume and FDG uptake in BA28 combined as dependent variables. Dichotomized spatial navigation (VS-ECog) performance and *APOE4* carrier status (positive or negative) were included as fixed factors. Age at PET, years of education, and overall cognitive performance (ADAS-cog-13) were included as covariates. The dichotomization of the VS-ECog was achieved by the median split of the VS-ECog sum score (impaired: VS-ECog sum score >2, normal or relatively preserved: VS-ECog sum score ≤2). Estimated marginal means are given as mean ± standard error (95%-confidence interval). Each two-way MANCOVA was complemented by two follow-up two-way univariate analyses of covariance (ANCOVA) to test specifically for the effect of either FDG uptake or grey matter volume alone. ("$p = 0.000$" means "$p < 0.0005$")

		Estimated marginal mean		Box's test / Levene's test		VS-ECog		*APOE4*		VS-ECog* *APOE4*		Age		ADAS-cog-13		Education	
		Impaired ($n = 147$)	normal ($n = 232$)	F	*p*	F	*p*	F	*p*	F	*p*	F	*p*	F	*p*	F	p
BA34	MANCOVA			0.592	0.805	2.551	0.079	0.916	0.401	1.308	0.272	41.077	**0.000**	16.441	**0.000**	3.645	**0.027**
	ANCOVA grey matter	0.868 ± 0.011 (0.845–0.890)	0.898 ± 0.009 (0.881–0.916)	0.519	0.670	4.405	**0.037**	0.075	0.785	0.344	0.558	82.367	**0.000**	26.931	**0.000**	3.545	0.061
	ANCOVA FDG	1.110 ± 0.010 (1.089–1.130)	1.102 ± 0.008 (1.086–1.118)	0.605	0.612	0.355	0.552	1.657	0.199	2.456	0.118	0.900	0.343	9.232	**0.003**	4.597	**0.033**
BA28	MANCOVA			1.354	0.203	2.362	0.096	1.640	0.195	1.280	0.279	30.902	**0.000**	25.053	**0.000**	2.908	0.056
	ANCOVA grey matter	1.062 ± 0.013 (1.037–1.088)	1.089 ± 0.010 (1.068–1.109)	0.810	0.489	2.418	0.121	0.407	0.524	2.374	0.124	60.834	**0.000**	35.180	**0.000**	4.369	**0.037**
	ANCOVA FDG	1.107 ± 0.011 (1.086–1.128)	1.094 ± 0.009 (1.077–1.110)	2.026	0.110	0.889	0.344	1.979	0.160	0.820	0.366	12.198	**0.001**	30.986	**0.000**	3.282	0.071

and neurodegeneration in BA34. This was demonstrated by a significant negative contribution of BA34 grey matter volume in the regression of the VS-ECog sum score. It was confirmed by lower BA34 grey matter volume in MCI patients with spatial navigation deficits (increased VS-ECog sum score) compared to MCI patients with relatively preserved spatial navigation. Statistical testing not only accounted for *APOE4* carrier status, age, and education, but also for overall cognitive performance (ADAS-cog-13) suggesting that volume loss of BA34 is associated with pronounced impairment specifically in spatial navigation. Moreover, the VS-ECog sum score was not significantly associated with grey matter volume in BA28 suggesting that spatial navigation is specifically sensitive to degeneration of BA34.

These findings are in line with the hypothesis of the study and, therefore, complement previous functional imaging studies by providing further lesion-based evidence for the association between BA34 integrity and spatial navigation in humans.

However, decision tree analysis of the dichotomized VS-ECog sum score with grey matter volume in BA34, age, and ADAS-cog-13 as predictors selected the grey matter volume in BA34 for branching at the root level, but the final model failed to improve on majority class prediction in the test set. This indicates that grey matter volume in BA34 is only a very weak predictor of spatial navigation performance.

Regression of the VS-ECog sum score did not reveal a significant contribution of FDG uptake in BA34, in contrast to the study hypothesis stating that reduced FDG uptake in BA34 might be an independent (of BA34 grey matter volume) predictor of spatial navigation performance. The rationale for this hypothesis was that synaptic dysfunction typically occurs before cell death [36]. Thus, some MCI patients might show reduced FDG uptake in BA34 despite normal grey matter volume. Potential explanations for the lack of association between VS-ECog and FDG uptake in BA34 include error amplification by partial volume correction [37]. The additional between-subject variability caused by error amplification might have prevented the detection of a possible association. There are several other factors that might have contributed to the lack of significant association between FDG uptake in BA34 and spatial navigation skills. First, about 75% of the glucose consumption in brain grey matter is associated with signaling-related synaptic activity [1, 38, 39]. As a consequence, loss of neurons in a given brain

region affects FDG uptake not only locally within this region, but the corresponding loss of efferent connections also causes reduced FDG uptake in distant brain regions innervated by axon fibers originating from the brain region affected by neuron loss. This complicates not only the interpretation of regional alterations of FDG uptake but also the interpretation of the lack of regional alterations. Second, while the FDG uptake pattern in the brain is very sensitive to alterations of brain synaptic activity [40–42], it is not specific to any given type of synaptic activity, in particular, it does not differentiate between excitatory and inhibitory activity. As a consequence, FDG-PET might not detect an imbalance of neuronal excitation versus inhibition as long as the total firing rate in the region is more or less unchanged. Studies in mouse models suggest that spatial navigation deficits are associated with an imbalance of neuronal excitation versus inhibition in the medial ERC [43]. Finally, altered coupling to other brain regions might cause compensatory changes associated with local hypermetabolism that might mask local degeneration in FDG-PET [44, 45]. MRI-based volumetry is less sensitive to at-distance and / or compensatory effects. However, given the large number of MCI subjects included in the present study, the lack of a significant contribution of BA34 FDG uptake to the VS–ECog regression indicates that FDG uptake in BA34 is at best a very weak independent predictor of spatial navigation performance.

A secondary finding of the present study was the association of spatial navigation performance with age. It should be noted that the negative sign of the age coefficient in the regression model of the VS-ECog sum score implies more strongly impaired spatial navigation in younger MCI patients, which might appear counter intuitive. A possible explanation would be multicollinearity of the predictor variables in the regression model, which would limit the interpretation of the regression coefficients of individual predictor variables. However, analysis of multicollinearity of grey matter volume in BA34, age, and ADAS-cog-13 did not reveal a severe multicollinearity problem among these variables: the variance inflation factors were considerably below commonly recommended thresholds of 5–10 (1.42, 1.32, and 1.17 for grey matter volume in BA34, age, and ADAS-cog-13, respectively). As a consequence, the results of the regression analysis can be considered valid not only with respect to the power of the whole model but also with respect to the contribution of individual predictors. Thus, the results of the regression analysis indicate more strongly impaired spatial navigation in younger compared to older MCI patients with the same degree of BA34 atrophy and the same level of overall cognitive impairment. This might be explained by a difference in the profile of cognitive impairment between younger and older MCI patients, with impairment of spatial navigation being *relatively* more pronounced compared to other cognitive domains in younger MCI patients. Spatial navigation performance did not differ between younger and older MCI patients in *absolut*e terms (Pearson correlation coefficient between "continuous" VS-ECog sum score and age in the whole sample = –0.019, $p = 0.719$). Another possible explanation of the negative partial correlation of the self-reported VS-ECog sum score with age is reduced awareness of impaired spatial navigation performance in older MCI patients. Lithfous and co-workers demonstrated an age-related decline of allocentric orientation but not of egocentric coding [46]. While the allocentric concept refers to the object-centered orientation and depends on attention, perception, and executive function, the egocentric orientation is self-centered and seems less affected in elderly patients [46]. However, the VS-ECog score employed in the present study does not explicitly distinguish between allocentric and egocentric orientation, thus limiting any inference of our findings in this regard.

APOE4 carriers have been reported to present lower density of grid cells in the ERC and altered spatial navigation years before onset of cognitive impairment [47]. The present study did not find an effect of *APOE4*-positivity on navigation performance or gray matter volume in BA34. *APOE4*-positivity may actually be considered a proxy for underlying AD in MCI. Thus, this finding would suggest that the association between BA34 degeneration and spatial navigation is not specific for AD. Several other age-related neurodegenerative pathologies, most notably primary age-related tauopathy, limbic-predominant age-related TDP-43 encephalopathy, and argyrophilic grain disease, also affect ERC integrity and can result in MCI [24, 48] including MCI phenotypes with prominent spatial navigation deficits [23, 49].

Clinical implications

Based on the association between VS-ECog and BA34 grey matter volume, the VS-ECog might be used as a screening tool to detect volume loss in

BA34. However, the VS-ECog sum score explained only 0.4% of the variance of BA34 grey matter volume beyond age, ADAS-cog-13, and TIV. This demonstrates that the VS-ECog provides only very limited independent information to predict BA34 atrophy in MCI patients.

Limitations

Limitations of the present study include its retrospective nature and the use of self-reported VS-ECog scores to characterize spatial navigation performance, which most likely is less reliable (in particular less sensitive) than specific tests of navigation performance [50]. This might have resulted in underestimation of the association between navigation performance and BA34 grey matter volume. Furthermore, the VS-ECog does not account for the complexity of spatial navigation in humans. For example, horizontal navigation relies more on visual inputs, while vertical navigation is managed mainly by the vestibular multisensory cortex [51]. A further limitation of this study is the use of spatial registration to map standard BA masks predefined in MNI space to the individual patient space for regional analysis. This approach provides only limited localization accuracy, particularly in case of strongly atrophic brains [52]. The resulting variability of no interest presumably reduced the power to detect effects and, therefore, might also have contributed to the failure to detect an association between spatial navigation performance and PVE corrected FDG uptake in BA34.

Conclusion

This study complements experimental animal research and human functional imaging studies by providing lesion-based evidence that impaired spatial navigation performance is associated with BA34 atrophy. The association is weak and, therefore, most likely is not useful in clinical routine patient care.

ACKNOWLEDGMENTS

Michel Grothe is supported by the "Miguel Servet" program [CP19/00031] of the Spanish Instituto de Salud Carlos III (ISCIIIFEDER).

Data collection and sharing for this project was funded by the Alzheimer's Disease Neuroimaging Initiative (ADNI) (National Institutes of Health Grant U01 AG024904) and DOD ADNI (Department of Defense award number W81XWH-12-2-0012). ADNI is funded by the National Institute on Aging, the National Institute of Biomedical Imaging and Bioengineering, and through generous contributions from the following: AbbVie, Alzheimer's Association; Alzheimer's Drug Discovery Foundation; Araclon Biotech; BioClinica, Inc.; Biogen; Bristol-Myers Squibb Company; CereSpir, Inc.; Cogstate; Eisai Inc.; Elan Pharmaceuticals, Inc.; Eli Lilly and Company; EuroImmun; F. Hoffmann-La Roche Ltd and its affiliated company Genentech, Inc.; Fujirebio; GE Healthcare; IXICO Ltd.; Janssen Alzheimer Immunotherapy Research & Development, LLC.; Johnson & Johnson Pharmaceutical Research & Development LLC.; Lumosity; Lundbeck; Merck & Co., Inc.; Meso Scale Diagnostics, LLC.; NeuroRx Research; Neurotrack Technologies; Novartis Pharmaceuticals Corporation; Pfizer Inc.; Piramal Imaging; Servier; Takeda Pharmaceutical Company; and Transition Therapeutics. The Canadian Institutes of Health Research is providing funds to support ADNI clinical sites in Canada. Private sector contributions are facilitated by the Foundation for the National Institutes of Health (www.fnih.org). The grantee organization is the Northern California Institute for Research and Education, and the study is coordinated by the Alzheimer's Therapeutic Research Institute at the University of Southern California. ADNI data are disseminated by the Laboratory for Neuro Imaging at the University of Southern California.

Authors' disclosures available online (https://www.j-alz.com/manuscript-disclosures/20-0520r3).

SUPPLEMENTARY MATERIAL

The supplementary material is available in the electronic version of this article: https://dx.doi.org/10.3233/JAD200520.

REFERENCES

[1] Sokoloff L (1999) Energetics of functional activation in neural tissues. *Neurochem Res* **24**, 321-329.

[2] Teipel S, Drzezga A, Grothe MJ, Barthel H, Chetelat G, Schuff N, Skudlarski P, Cavedo E, Frisoni GB, Hoffmann W, Thyrian JR, Fox C, Minoshima S, Sabri O, Fellgiebel A (2015) Multimodal imaging in Alzheimer's disease: Validity and usefulness for early detection. *Lancet Neurol* **14**, 1037-1053.

[3] Young PNE, Estarellas M, Coomans E, Srikrishna M, Beaumont H, Maass A, Venkataraman AV, Lissaman R, Jimenez D, Betts MJ, McGlinchey E, Berron D, O'Connor A,

Fox NC, Pereira JB, Jagust W, Carter SF, Paterson RW, Scholl M (2020) Imaging biomarkers in neurodegeneration: Current and future practices. *Alzheimers Res Ther* **12**, 49.

[4] Amoroso N, Rocca M, Bellotti R, Fanizzi A, Monaco A, Tangaro S (2018) Alzheimer's disease diagnosis based on the Hippocampal Unified Multi-Atlas Network (HUMAN) algorithm. *Biomed Eng Online* **17**, 6.

[5] Sarica A, Vasta R, Novellino F, Vaccaro MG, Cerasa A, Quattrone A (2018) MRI asymmetry index of hippocampal subfields increases through the continuum from the mild cognitive impairment to the Alzheimer's disease. *Front Neurosci* **12**, 576.

[6] El Haj M, Colombel F, Kapogiannis D, Gallouj K (2020) False memory in Alzheimer's disease. *Behav Neurol* **2020**, 5284504.

[7] Lisman J, Buzsaki G, Eichenbaum H, Nadel L, Ranganath C, Redish AD (2017) Viewpoints: How the hippocampus contributes to memory, navigation and cognition. *Nat Neurosci* **20**, 1434-1447.

[8] Budson AE, Solomon PR (2017) *Memory Loss, Alzheimer's Disease, and Dementia: A Practical Guide for Clinicians*, Elsevier Inc.

[9] Lombardi G, Crescioli G, Cavedo E, Lucenteforte E, Casazza G, Bellatorre AG, Lista C, Costantino G, Frisoni G, Virgili G, Filippini G (2020) Structural magnetic resonance imaging for the early diagnosis of dementia due to Alzheimer's disease in people with mild cognitive impairment. *Cochrane Database Syst Rev* **3**, CD009628.

[10] Munoz M, Insausti R (2005) Cortical efferents of the entorhinal cortex and the adjacent parahippocampal region in the monkey (Macaca fascicularis). *Eur J Neurosci* **22**, 1368-1388.

[11] Maass A, Berron D, Libby LA, Ranganath C, Duzel E (2015) Functional subregions of the human entorhinal cortex. *Elife* **4**, e06426.

[12] Navarro Schroder T, Haak KV, Zaragoza Jimenez NI, Beckmann CF, Doeller CF (2015) Functional topography of the human entorhinal cortex. *Elife* **4**, e06738.

[13] Fyhn M, Molden S, Witter MP, Moser EI, Moser MB (2004) Spatial representation in the entorhinal cortex. *Science* **305**, 1258-1264.

[14] Hafting T, Fyhn M, Molden S, Moser MB, Moser EI (2005) Microstructure of a spatial map in the entorhinal cortex. *Nature* **436**, 801-806.

[15] Sargolini F, Fyhn M, Hafting T, McNaughton BL, Witter MP, Moser MB, Moser EI (2006) Conjunctive representation of position, direction, and velocity in entorhinal cortex. *Science* **312**, 758-762.

[16] Tsao A, Sugar J, Lu L, Wang C, Knierim JJ, Moser MB, Moser EI (2018) Integrating time from experience in the lateral entorhinal cortex. *Nature* **561**, 57-62.

[17] Habets AM, Lopes Da Silva FH, Mollevanger WJ (1980) An olfactory input to the hippocampus of the cat: Field potential analysis. *Brain Res* **182**, 47-64.

[18] Kerr KM, Agster KL, Furtak SC, Burwell RD (2007) Functional neuroanatomy of the parahippocampal region: The lateral and medial entorhinal areas. *Hippocampus* **17**, 697-708.

[19] Insausti R, Corcoles-Parada M, Ubero MM, Rodado A, Insausti AM, Munoz-Lopez M (2019) Cytoarchitectonic areas of the gyrus ambiens in the human brain. *Front Neuroanat* **13**, 12.

[20] Petersen RC, Smith GE, Ivnik RJ, Tangalos EG, Schaid DJ, Thibodeau SN, Kokmen E, Waring SC, Kurland LT (1995) Apolipoprotein-E status as a predictor of the development of Alzheimer's disease in memory-impaired individuals. *JAMA* **273**, 1274-1278.

[21] Golomb J, Kluger A, Ferris SH (2004) Mild cognitive impairment: Historical development and summary of research. *Dialogues Clin Neurosci* **6**, 351-367.

[22] Hort J, Laczo J, Vyhnalek M, Bojar M, Bures J, Vlcek K (2007) Spatial navigation deficit in amnestic mild cognitive impairment. *Proc Natl Acad Sci U S A* **104**, 4042-4047.

[23] Howett D, Castegnaro A, Krzywicka K, Hagman J, Marchment D, Henson R, Rio M, King JA, Burgess N, Chan D (2019) Differentiation of mild cognitive impairment using an entorhinal cortex-based test of virtual reality navigation. *Brain* **142**, 1751-1766.

[24] Abner EL, Kryscio RJ, Schmitt FA, Fardo DW, Moga DC, Ighodaro ET, Jicha GA, Yu L, Dodge HH, Xiong C, Woltjer RL, Schneider JA, Cairns NJ, Bennett DA, Nelson PT (2017) Outcomes after diagnosis of mild cognitive impairment in a large autopsy series. *Ann Neurol* **81**, 549-559.

[25] Pennanen C, Kivipelto M, Tuomainen S, Hartikainen P, Hanninen T, Laakso MP, Hallikainen M, Vanhanen M, Nissinen A, Helkala EL, Vainio P, Vanninen R, Partanen K, Soininen H (2004) Hippocampus and entorhinal cortex in mild cognitive impairment and early AD. *Neurobiol Aging* **25**, 303-310.

[26] Farias ST, Mungas D, Reed BR, Cahn-Weiner D, Jagust W, Baynes K, Decarli C (2008) The measurement of everyday cognition (ECog): Scale development and psychometric properties. *Neuropsychology* **22**, 531-544.

[27] Ashburner J, Friston KJ (2005) Unified segmentation. *Neuroimage* **26**, 839-851.

[28] Herron TJ, Kang XJ, Woods DL (2012) Automated measurement of the human corpus callosum using MRI. *Front Neuroinform* **6**, 25.

[29] Lancaster JL, Woldorff MG, Parsons LM, Liotti M, Freitas CS, Rainey L, Kochunov PV, Nickerson D, Mikiten SA, Fox PT (2000) Automated Talairach atlas labels for functional brain mapping. *Hum Brain Mapp* **10**, 120-131.

[30] Maldjian JA, Laurienti PJ, Kraft RA, Burdette JH (2003) An automated method for neuroanatomic and cytoarchitectonic atlas-based interrogation of fMRI data sets. *Neuroimage* **19**, 1233-1239.

[31] Lange C, Suppa P, Frings L, Brenner W, Spies L, Buchert R (2016) Optimization of statistical single subject analysis of brain FDG PET for the prognosis of mild cognitive impairment-to-Alzheimer's disease conversion. *J Alzheimers Dis* **49**, 945-959.

[32] Andersson JL, Vagnhammar BE, Schneider H (1995) Accurate attenuation correction despite movement during PET imaging. *J Nucl Med* **36**, 670-678.

[33] Gonzalez-Escamilla G, Lange C, Teipel S, Buchert R, Grothe MJ, Alzheimer's Disease Neuroimaging Initiative (2017) PETPVE12: An SPM toolbox for Partial Volume Effects correction in brain PET - Application to amyloid imaging with AV45-PET. *Neuroimage* **147**, 669-677.

[34] Minoshima S, Frey KA, Foster NL, Kuhl DE (1995) Preserved pontine glucose metabolism in Alzheimer disease: A reference region for functional brain image (PET) analysis. *J Comput Assist Tomogr* **19**, 541-547.

[35] Maguire EA, Burgess N, O'Keefe J (1999) Human spatial navigation: Cognitive maps, sexual dimorphism, and neural substrates. *Curr Opin Neurobiol* **9**, 171-177.

[36] Selkoe DJ (2002) Alzheimer's disease is a synaptic failure. *Science* **298**, 789-791.

[37] Erlandsson K, Buvat I, Pretorius PH, Thomas BA, Hutton BF (2012) A review of partial volume correction techniques for emission tomography and their applications in neurology, cardiology and oncology. *Phys Med Biol* **57**, R119-159.

[38] Kadekaro M, Crane AM, Sokoloff L (1985) Differential effects of electrical stimulation of sciatic nerve on metabolic activity in spinal cord and dorsal root ganglion in the rat. *Proc Natl Acad Sci U S A* **82**, 6010-6013.

[39] Attwell D, Laughlin SB (2001) An energy budget for signaling in the grey matter of the brain. *J Cereb Blood Flow Metab* **21**, 1133-1145.

[40] Phelps ME, Mazziotta JC, Kuhl DE, Nuwer M, Packwood J, Metter J, Engel J, Jr. (1981) Tomographic mapping of human cerebral metabolism visual stimulation and deprivation. *Neurology* **31**, 517-529.

[41] Mazziotta JC, Phelps ME, Halgren E (1983) Local cerebral glucose metabolic response to audiovisual stimulation and deprivation: Studies in human subjects with positron CT. *Hum Neurobiol* **2**, 11-23.

[42] Wang GJ, Volkow ND, Telang F, Jayne M, Ma Y, Pradhan K, Zhu W, Wong CT, Thanos PK, Geliebter A, Biegon A, Fowler JS (2009) Evidence of gender differences in the ability to inhibit brain activation elicited by food stimulation. *Proc Natl Acad Sci U S A* **106**, 1249-1254.

[43] Fu HJ, Rodriguez GA, Herman M, Emrani S, Nahmani E, Barrett G, Figueroa HY, Goldberg E, Hussaini SA, Duff KE (2017) Tau pathology induces excitatory neuron loss, grid cell dysfunction, and spatial memory deficits reminiscent of early Alzheimer's disease. *Neuron* **93**, 533-541.e5,

[44] Apostolova I, Lange C, Maurer A, Suppa P, Spies L, Grothe MJ, Nierhaus T, Fiebach JB, Steinhagen-Thiessen E, Buchert R, Alzheimer's Disease Neuroimaging Initiative (2018) Hypermetabolism in the hippocampal formation of cognitively impaired patients indicates detrimental maladaptation. *Neurobiol Aging* **65**, 41-50.

[45] Tahmasian M, Pasquini L, Scherr M, Meng C, Forster S, Bratec SM, Shi KY, Yakushev I, Schwaiger M, Grimmer T, Diehl-Schmid J, Riedl V, Sorg C, Drzezga A (2015) The lower hippocampus global connectivity, the higher its local metabolism in Alzheimer disease. *Neurology* **84**, 1956-1963.

[46] Lithfous S, Dufour A, Blanc F, Despres O (2014) Allocentric but not egocentric orientation is impaired during normal aging: An ERP study. *Neuropsychology* **28**, 761-771.

[47] Kunz L, Schroder TN, Lee H, Montag C, Lachmann B, Sariyska R, Reuter M, Stirnberg R, Stocker T, Messing-Floeter PC, Fell J, Doeller CF, Axmacher N (2015) Reduced grid-cell-like representations in adults at genetic risk for Alzheimer's disease. *Science* **350**, 430-433.

[48] Nelson PT, Dickson DW, Trojanowski JQ, Jack CR, Boyle PA, Arfanakis K, Rademakers R, Alafuzoff I, Attems J, Brayne C, Coyle-Gilchrist ITS, Chui HC, Fardo DW, Flanagan ME, Halliday G, Hokkanen SRK, Hunter S, Jicha GA, Katsumata Y, Kawas CH, Keene CD, Kovacs GG, Kukull WA, Levey AI, Makkinejad N, Montine TJ, Murayama S, Murray ME, Nag S, Rissman RA, Seeley WW, Sperling RA, White Iii CL, Yu L, Schneider JA (2019) Limbic-predominant age-related TDP-43 encephalopathy (LATE): Consensus working group report. *Brain* **142**, 1503-1527.

[49] Stangl M, Achtzehn J, Huber K, Dietrich C, Tempelmann C, Wolbers T (2018) Compromised grid-cell-like representations in old age as a key mechanism to explain age-related navigational deficits. *Curr Biol* **28**, 1108-1115.e6.

[50] Pal A, Biswas A, Pandit A, Roy A, Guin D, Gangopadhyay G, Senapati AK (2016) Study of visuospatial skill in patients with dementia. *Ann Indian Acad Neur* **19**, 83-88.

[51] Zwergal A, Schoberl F, Xiong G, Pradhan C, Covic A, Werner P, Trapp C, Bartenstein P, la Fougere C, Jahn K, Dieterich M, Brandt T (2016) Anisotropy of human horizontal and vertical navigation in real space: Behavioral and PET correlates. *Cereb Cortex* **26**, 4392-4404.

[52] Fischl B, Stevens AA, Rajendran N, Yeo BTT, Greve DN, Van Leemput K, Polimeni JR, Kakunoori S, Buckner RL, Pacheco J, Salat DH, Melcher J, Frosch MP, Hyman BT, Grant PE, Rosen BR, van der Kouwe AJW, Wiggins GC, Wald LL, Augustinack JC (2009) Predicting the location of entorhinal cortex from MRI. *Neuroimage* **47**, 8-17.